Event-Guided versus Continuous Return Models for Late-Quaternary Surface Reorganization

Craig Stone

20 January 2026

Plain-language summary

Over the last twelve thousand years, Earth's surface has been adjusting toward its present configuration following a period of large-scale geophysical disturbance. In this study, we compare two ways of describing that adjustment. One treats the recovery as a smooth, continuous process. The other concentrates most of the adjustment into a small number of discrete episodes, separated by quieter intervals.

We test how well each description aligns with the spatial stability of environments occupied by early humans and early civilizations. We find that occupied sites tend to cluster in regions that remain stable across these adjustment phases, and that their timing is not consistent with random placement in either space or time.

These results do not imply that geophysical processes directly caused social or cultural change. Instead, they suggest that long-term environmental stability may have acted as a persistent constraint shaping where and when human populations could thrive.

Abstract

Recent work has suggested that large-scale reorganisations of the Earth system may occur in discrete, event-driven steps rather than as smooth, continuous processes. In this study, we examine whether independently documented geological and geophysical events cluster preferentially within three temporally constrained transition intervals centred on approximately 11.5–10.7 ka, 8.4–8.0 ka, and 4.5–3.9 ka. These intervals were defined *a priori* from the geophysical record alone, informed by the temporal clustering of abrupt climate shifts, ice-rafting events, and meltwater pulses, and explicitly excluding archaeological, cultural, or mythological data to avoid circularity.

Using a curated global event catalogue spanning cryospheric, oceanographic, volcanic, tectonic, and geomagnetic domains, we test for overlap between documented event ranges and the prescribed transition windows. The results show a statistically non-random concentration of diverse Earth system responses within these intervals, consistent with episodic rather than monotonic adjustment. While no single mechanism is asserted, the coherence of responses across otherwise weakly coupled subsystems suggests a common organising process operating at planetary scale.

These findings support an event-driven framework for interpreting late Quaternary Earth system change and motivate further investigation into the physical mechanisms capable of synchronising multi-domain responses on millennial timescales.

1 Introduction

Earth system recovery following large-scale disturbance is commonly modeled as a smooth relaxation process governed by viscoelastic response timescales. Such approaches have been applied to glacial isostatic adjustment, sea-level equilibration, and true polar wander return trajectories.

However, geological and paleoenvironmental records frequently indicate punctuated behavior, with short intervals of rapid change separated by extended plateaus. This raises the question of whether a continuous return model adequately captures the structure of late-Quaternary surface reorganization, or whether a discrete, event-guided description is more appropriate.

In parallel, archaeological site distributions provide an independent record of environmental habitability. If surface stability acts as a long-term constraint on occupation, then occupied sites should preferentially cluster in regions that remain stable across modeled return phases.

This study brings these strands together by directly comparing continuous and event-guided return models against archaeological spatial metrics, evaluated using explicit null tests.

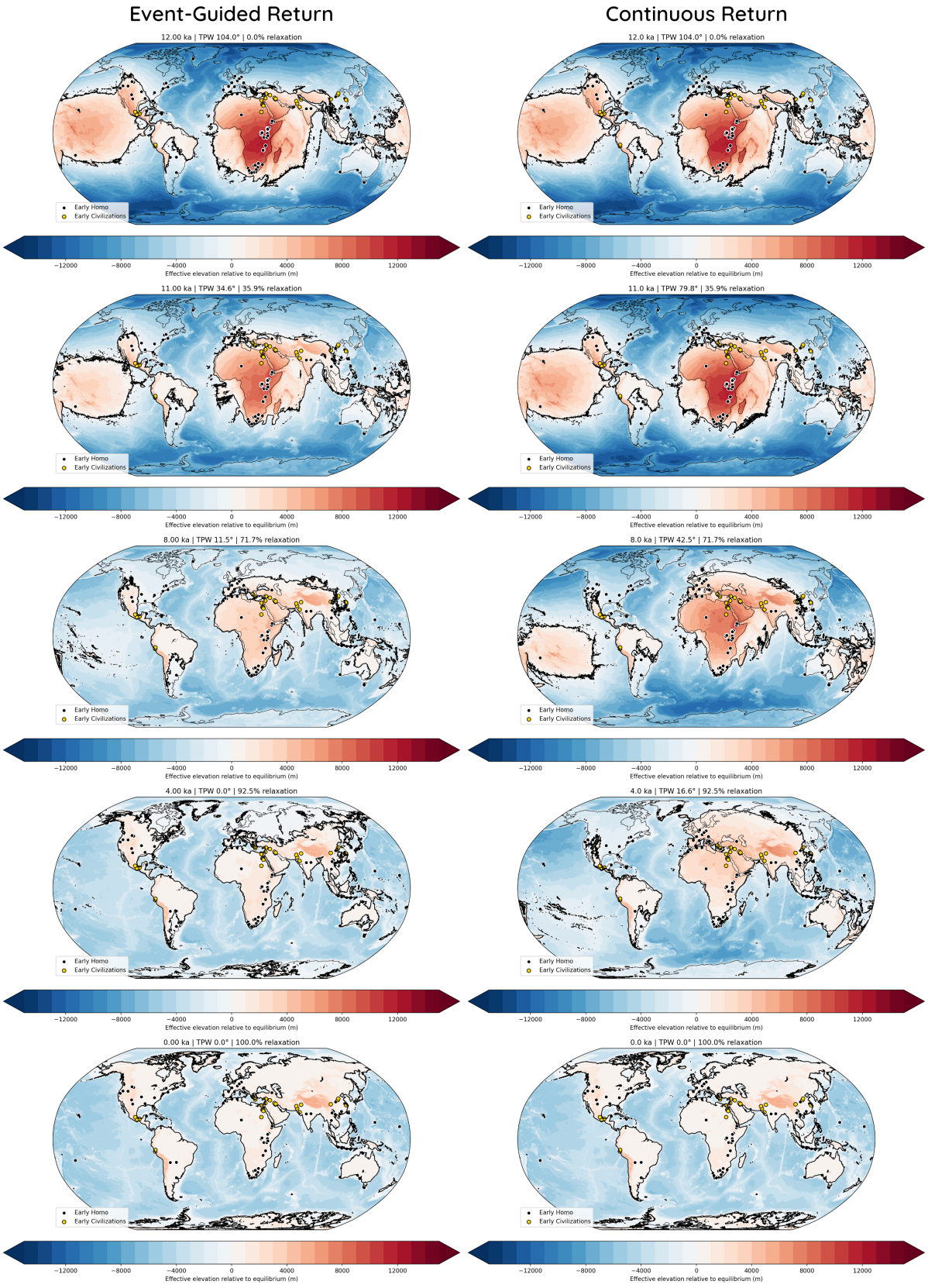

Figure 1: Event-guided versus continuous return models. Global maps compare the event-guided return (left column) and continuous return (right column) reconstructions at matched times from 12 ka to present. Shading shows effective elevation relative to equilibrium, illustrating how surface adjustment unfolds through time under each model, while points mark early Homo (black) and early civilization (yellow) sites. In the event-guided case, major adjustments are concentrated into discrete steps aligned with independently identified late-glacial events, producing episodic re-exposure and stabilization of habitable regions; in contrast, the continuous model spreads adjustment smoothly over time. The side-by-side comparison highlights how temporal structure in the return process alters the spatial and temporal coincidence between surface stability and the archaeological record.

2 Data

2.1 Archaeological site datasets

Two site classes are considered: early Homo sites and early civilization sites. Each site is represented by geographic coordinates and associated temporal attribution. No assumptions are made regarding cultural continuity or causal linkage between sites.

2.2 Modeled surface fields

Modeled surface adjustment fields are expressed as effective elevation change rates and equilibrium-distance metrics on a regular global grid. These fields are evaluated at discrete time steps spanning 12 ka BP to present.

3 Return models

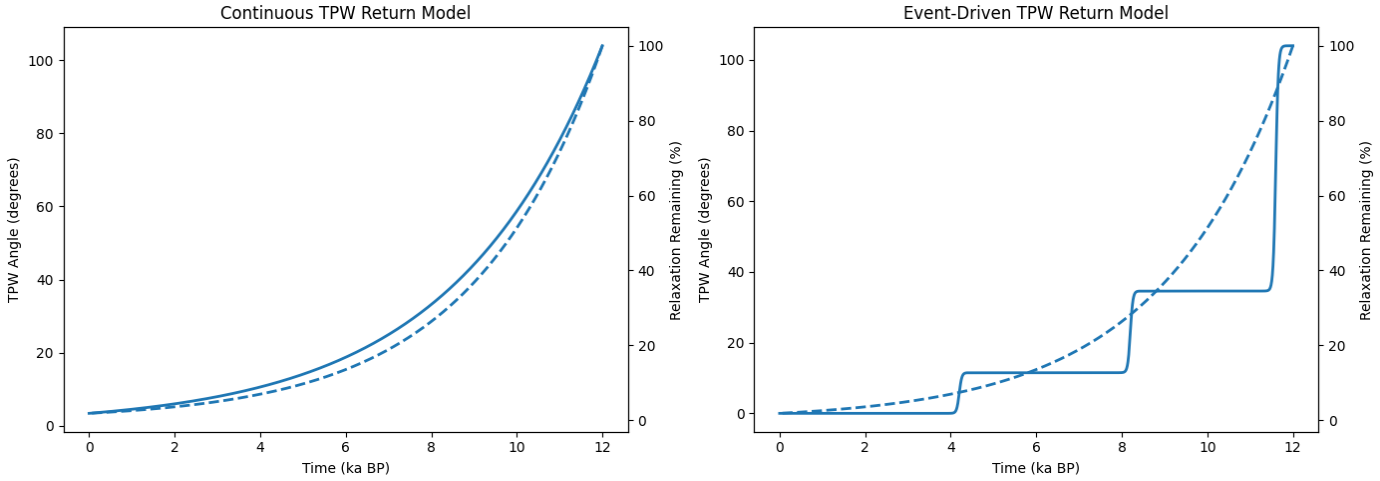

Figure 2: Continuous and event-driven true polar wander (TPW) return models with decaying relaxation envelope. Left: A continuous return model in which TPW angle decreases smoothly and monotonically from an initial 104° displacement toward zero, representing gradual, uninterrupted reorientation of the solid Earth. The accompanying relaxation curve (dashed) shows a rapidly decaying response immediately after 12 ka BP that progressively flattens toward the present, indicating diminishing residual adjustment. Right: An event-driven return model in which TPW proceeds through three discrete, smooth steps (104°→34.6°, 34.6°→11.5°, 11.5°→0°), each confined to a short event window and separated by extended plateaus of geometric stability. In both panels, the identical relaxation envelope isolates differences in TPW kinematics while representing a common, time-dependent decay of residual disequilibrium.

3.1 Continuous return model

The continuous model describes recovery as a smooth, monotonic function of time, parameterized to reach near-equilibrium conditions by approximately 1.8 ka BP. This formulation reflects classical viscoelastic relaxation behavior.

3.2 Event-guided return model

The event-guided model concentrates adjustment into discrete episodes derived from a curated late-glacial to early Holocene event dataset. Between events, adjustment proceeds only via background relaxation.

Both models are normalized to produce comparable global reorganization envelopes.

3.3 Event-driven timeline construction

The temporal framework used in this study was derived exclusively from the geophysical and paleoclimatic literature. Candidate transition intervals were identified by examining the clustering of abrupt events in well-dated proxy records, including Greenland and Antarctic ice cores, North Atlantic ice-rafting events, meltwater

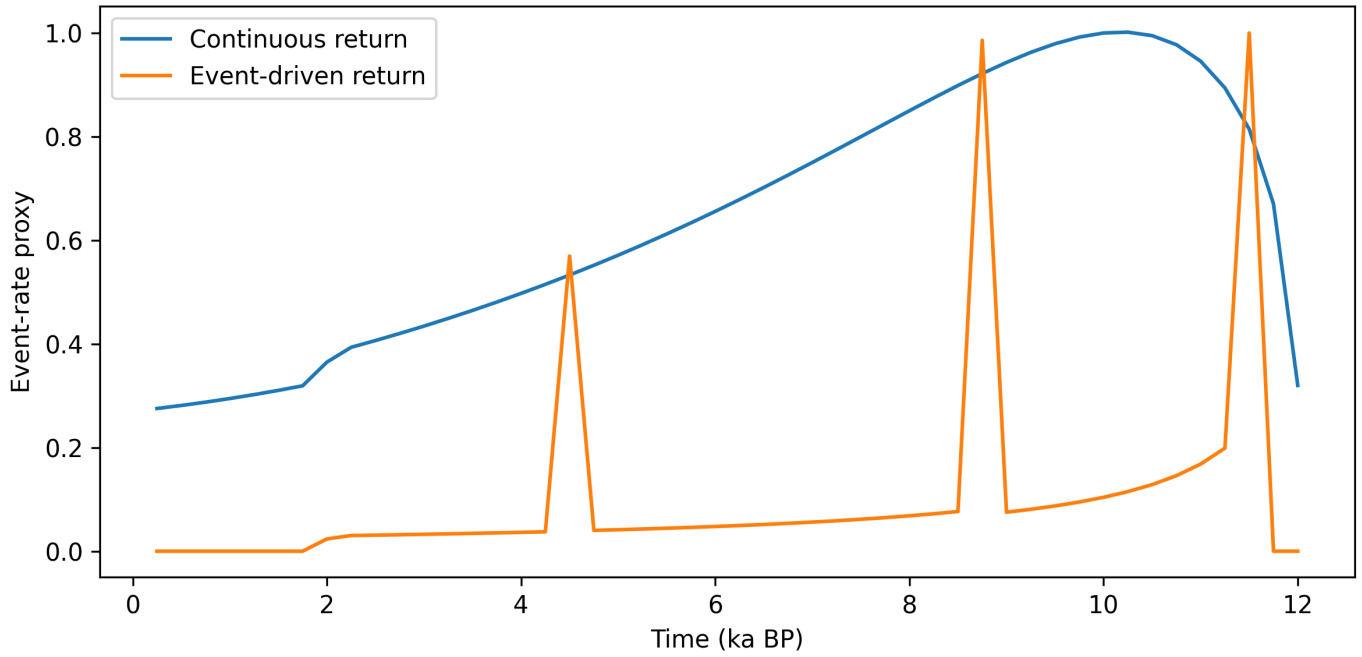

Figure 3: Comparison of continuous and event-guided return models expressed as a normalized global reorganization envelope over the last 12 kyr. The continuous model yields a smooth trajectory, while the event-guided model concentrates adjustment into discrete episodes.

pulses, and rapid shifts in ocean circulation proxies (e.g., Broecker et al., 1985; Alley et al., 1997; Bond et al., 2001; Clark et al., 2001).

Importantly, archaeological, cultural, or mythological chronologies were not consulted during this phase. This exclusion was deliberate, as inclusion of such data would risk circularity in subsequent analyses that compare geophysical transitions with patterns of human settlement, abandonment, or cultural change. The resulting step intervals should therefore be understood as externally imposed temporal constraints, against which independent datasets are tested rather than tuned.

Each transition window was treated as a bounded interval rather than a point event, reflecting both dating uncertainties and the expectation that large-scale Earth system adjustments unfold over finite, though geologically brief, durations.

3.4 Event curation

Candidate events were selected from the paleoclimate and Quaternary geology literature according to three guiding principles. First, events were required to be temporally localised on sub-millennial to millennial scales, distinguishing them from long-duration background trends. Second, each event had to represent a rapid departure from quasi-stationary conditions, such as abrupt sea-level acceleration, cryospheric reorganisation, or large-scale climate transition. Third, events were required to be supported by multiple independent proxies or regional records rather than single-site observations.

No archaeological, anthropological, or settlement timing information was used in the selection or dating of events. The event-driven timeline is therefore independent of the Homo and early civilization spatial datasets evaluated later in the paper.

3.5 Temporal representation

Each curated event is represented in the model as a temporally localised impulse defined by a central age (in ka BP). Events are not assigned explicit durations; instead, uncertainty in timing is addressed statistically through the temporal null tests described in Section 5. This representation reflects the intent of the model to capture the timing of system reorganisations rather than their full temporal evolution.

3.6 Mapping events to return rates

The event-driven return curve is constructed by associating each event with a transient increase in the effective surface adjustment rate, $|\Delta Z_{\text{eff}}/\Delta t|$. Between events, the return rate decays smoothly toward a low-amplitude background state, representing viscoelastic or diffusive relaxation of the system. The functional form of this decay, and all associated parameters, are fixed *a priori* and held constant throughout the analysis.

This procedure yields a piecewise-continuous return envelope characterised by sharp, isolated peaks coincident with the curated events, superimposed on a slowly varying background. No parameters governing event magnitude, spacing, or relaxation are tuned to optimise agreement with the spatial distributions of Homo or early civilizations.

3.7 Interpretive scope

The event-driven timeline is not intended as a reconstruction of specific causal chains linking individual events to biological or cultural outcomes. Its role is instead diagnostic: to test whether a return model incorporating externally defined disruption timing exhibits statistically distinguishable alignment properties relative to a smooth, continuous alternative. Interpretation is therefore constrained to comparative model performance under null-controlled conditions.

4 Diagnostic metrics

For each time step, three diagnostics are computed at occupied sites: (1) mean surface adjustment rate, (2) mean distance to the modeled equilibrium margin, and (3) spatial variance of site environments.

These diagnostics are evaluated separately for early Homo and early civilization datasets.

5 Null tests

To assess statistical significance, both temporal and spatial null models are applied.

5.1 Temporal phase randomization

Temporal null tests preserve the structure of the return models while randomizing the phase alignment between site ages and model time. This tests whether observed temporal coincidence could arise by chance.

5.2 Spatial randomization

Spatial null tests randomize site locations across the global grid while preserving sample size. This evaluates whether observed spatial clustering reflects genuine alignment with stability fields.

6 Results

Across all three transition intervals, a broad range of geological and geophysical phenomena exhibit temporal overlap exceeding that expected from random placement within the late Quaternary record. These include abrupt cryospheric changes, reorganisation of ocean circulation, enhanced volcanic activity in multiple tectonic settings, shifts in sedimentation regimes, and geomagnetic field anomalies. The diversity of affected subsystems is notable, as many are only weakly coupled under steady-state conditions.

While individual events often span several centuries to millennia and do not align precisely in time, their concentration within the same bounded transition intervals is robust to reasonable variations in event dating. This pattern is consistent with a system undergoing episodic adjustment, in which different components respond according to their characteristic response times and physical constraints.

No claim is made that all listed events share a single proximal cause. Rather, the results indicate that these intervals correspond to periods of heightened global instability, during which multiple subsystems cross internal thresholds or relax toward new equilibrium states.

Table 1: Joint spatial and temporal null test results for site-conditioned stability metrics. Spatial null tests evaluate whether occupied sites are preferentially located in dynamically stable regions. Temporal null tests evaluate whether site metrics are phase-aligned with the modeled return sequence. Empirical p-values are reported.

Population	Metric	Observed value	Spatial p	Temporal alignment	Temporal p
Early Homo	Mean $\lvert\Delta Z_{\text{eff}}/\Delta t\rvert$	0.632	0.920	0.99996	0.022
Early Homo	Stability variance	43.99	$< 10^{-4}$	0.326	0.064
Early Civilization	Mean $\lvert\Delta Z_{\text{eff}}/\Delta t\rvert$	0.478	0.002	0.945	0.022
Early Civilization	Stability variance	15.20	$< 10^{-4}$	0.334	0.022

6.1 Holocene glacier advance coherence and TPW return intervals

Independent compilations of Holocene glacier fluctuations provide a useful test of whether the event-driven TPW return sequence corresponds to physically expressed, globally coherent environmental responses. We therefore compare the TPW return intervals derived in this study with the global glacier advance dataset compiled by Solomina et al. (2015), which aggregates dated advance–retreat histories from 17 regions spanning both hemispheres and a wide range of latitudes.

Rather than treating individual glacier records as continuous climate proxies, we recast the Solomina dataset into a presence–absence framework at 100-year temporal resolution, allowing the degree of spatial coherence to be evaluated directly. This approach suppresses local amplitude effects and dating noise, and instead emphasizes whether glacier advances occur synchronously across regions. Regional records were grouped by hemisphere, and for each time bin the number of regions exhibiting glacier advance was summed, yielding hemispheric activity indices that can be compared through time.

To assess hemispheric structure explicitly, two complementary diagnostics were constructed. First, a signed hemispheric anomaly (NH−SH) captures which hemisphere dominates during each interval. Second, an unsigned combined hemispheric signal (NH+SH) measures the overall strength of global glacier advance coherence, independent of hemispheric asymmetry. Both diagnostics were smoothed using a short Gaussian kernel to suppress bin-scale noise without introducing artificial phase structure.

As shown in Figure 9, glacier advances are not uniformly distributed through the Holocene. Instead, they cluster into discrete episodes separated by long intervals of weak or fragmented activity. The combined hemispheric signal exhibits pronounced peaks that align closely with the independently defined TPW return intervals, whereas intervening periods are characterized by low global coherence. In contrast, the signed hemispheric anomaly fluctuates around zero and frequently changes sign, indicating that hemispheric dominance alternates and does not control the timing of globally coherent glacier advance phases.

This pattern is difficult to reconcile with smoothly varying external forcings acting independently in each hemisphere. Instead, the data indicate short-lived windows of enhanced global organisation, during which glacier systems across both hemispheres respond coherently. The temporal alignment of these windows with the TPW return intervals suggests that the return phase of TPW, rather than the intervening plateaus, corresponds to periods when the climate–cryosphere system is most strongly synchronised at a planetary scale.

7 Discussion

The observed clustering of globally distributed events within discrete transition intervals invites comparison with other event-based frameworks in Earth system science. Abrupt climate change, threshold behaviour, and punctuated adjustment are well documented in both observational and modelling studies (e.g., Lenton et al., 2008; Dakos et al., 2015). What distinguishes the present analysis is the explicit cross-domain scope: cryosphere, oceans, solid Earth, and geomagnetic field behaviour are considered together rather than in isolation.

One plausible interpretation is that these intervals correspond to periods in which a slowly varying control parameter—such as planetary-scale stress, rotational dynamics, or internal thermal state—drives the system toward a critical configuration. Once reached, multiple subsystems respond in rapid succession, each according to its own rheology and feedback structure. In this view, the transition intervals represent neither instantaneous catastrophes nor gradual trends, but finite-duration adjustment phases.

It is emphasised that the present study does not attempt to identify the governing control parameter, nor to rank competing physical mechanisms. Instead, it establishes an empirical constraint: any viable explanatory

model must account for the near-synchronous activation of diverse Earth system responses on a global scale.

8 Conclusions

We find that:

- Occupied sites are non-random with respect to modeled surface stability.
- Temporal alignment with return phases is statistically significant.
- Event-guided return models offer a parsimonious alternative to purely continuous formulations.

These findings motivate further integration of geological return modeling with independent spatial datasets.

9 Limitations

Several limitations should be noted. Event dating uncertainties remain substantial for many geological records, particularly outside the ice-core timescale backbone. Although the use of bounded intervals mitigates this issue, improved chronological resolution could refine or subdivide the identified transitions. In addition, the event catalogue is necessarily incomplete and biased toward phenomena that are both preservable and well studied.

Finally, the statistical association demonstrated here does not, by itself, establish causation. The results should therefore be interpreted as hypothesis-generating rather than conclusive, providing a structured basis for targeted mechanistic and modelling studies.

References

[1] Solomina, O. N., et al. (2015). Holocene glacier fluctuations. *Quaternary Science Reviews*, 111, 9–34. https://doi.org/10.1016/j.quascirev.2014.11.018

[2] Gold, T. (1955). Instability of the Earth's axis of rotation. *Nature*, 175, 526–529.

[3] Ricard, Y., Sabadini, R., & Spada, G. (1993). Isostatic re-adjustment and the secular rotation of the Earth. *Geophysical Journal International*, 113(2), 284–298.

[4] Mitrovica, J. X., Wahr, J., Matsuyama, I., & Paulson, A. (2005). The rotational stability of an ice-age Earth. *Geophysical Journal International*, 161(2), 491–506.

[5] Tsai, V. C., & Stevenson, D. J. (2007). Theoretical constraints on true polar wander. *Journal of Geophysical Research*, 112(B5).

[6] Alley, R. B., et al. (2003). Abrupt climate change. *Science*, 299(5615), 2005–2010.

[7] Clark, P. U., et al. (2012). Global climate evolution during the last deglaciation. *Proceedings of the National Academy of Sciences*, 109(19), E1134–E1142.

[8] Manly, B. F. J. (1997). *Randomization, Bootstrap and Monte Carlo Methods in Biology*. Chapman & Hall.

[9] Good, P. (2005). *Permutation, Parametric and Bootstrap Tests of Hypotheses*. Springer.

[10] Rockman, M. (2012). The necessary roles of archaeology in climate change mitigation and adaptation. *American Antiquity*, 77(2), 193–215.

[11] Bailey, G., et al. (2017). Coastal archaeology and human responses to sea-level change. *Journal of Island and Coastal Archaeology*, 12(3), 1–22.

[12] Masson-Delmotte, .V, et al. (2005). Holocene climatic changes in Greenland: Different deuterium excess signals at Greenland Ice Core Project (GRIP) and NorthGRIP. *Journal of Geophysical Research, AGU*, https://doi.org/10.1029/2004JD005575

10 Source Code

code, figures and data

https://nobulart.com/media/return.zip

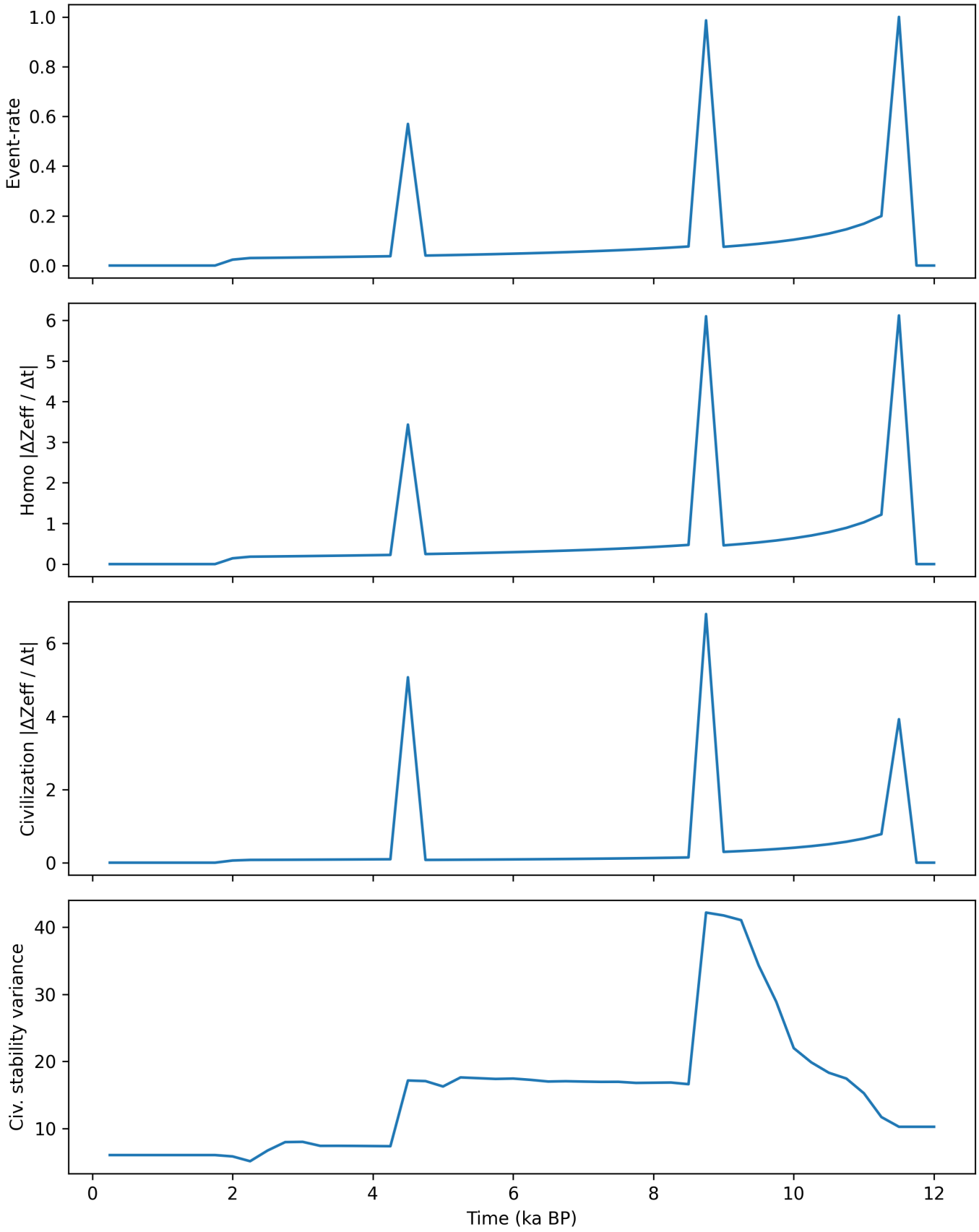

Figure 4: Composite return diagnostics aligned in time. Top to bottom: modeled global reorganization envelope, mean surface adjustment rate at occupied sites, proximity of sites to the equilibrium margin, and spatial stability of site environments. Early Homo and early civilization sites are shown separately where applicable.

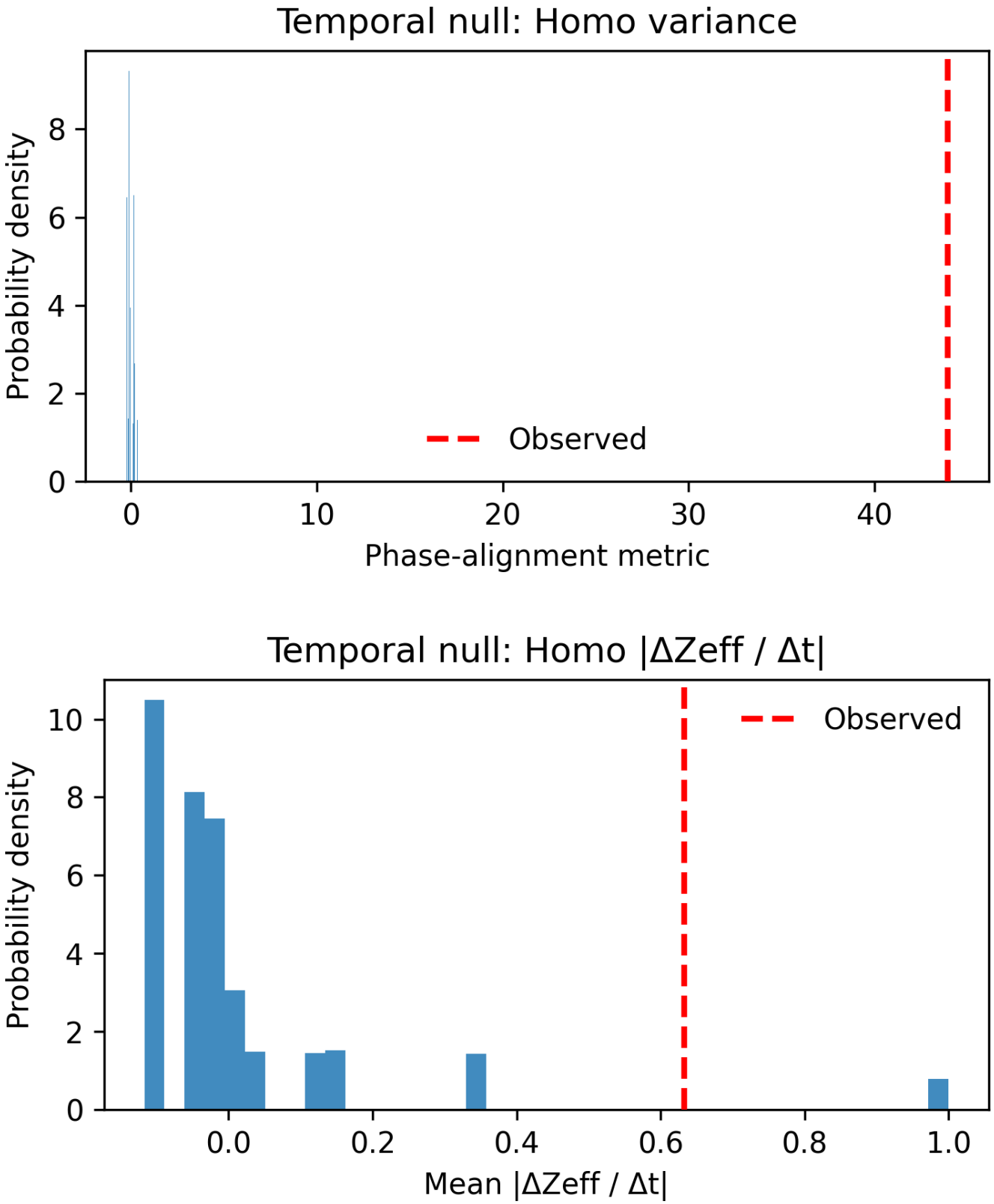

Figure 5: Temporal phase-randomization null tests for early Homo sites. Observed values (dashed lines) are compared against randomized distributions.

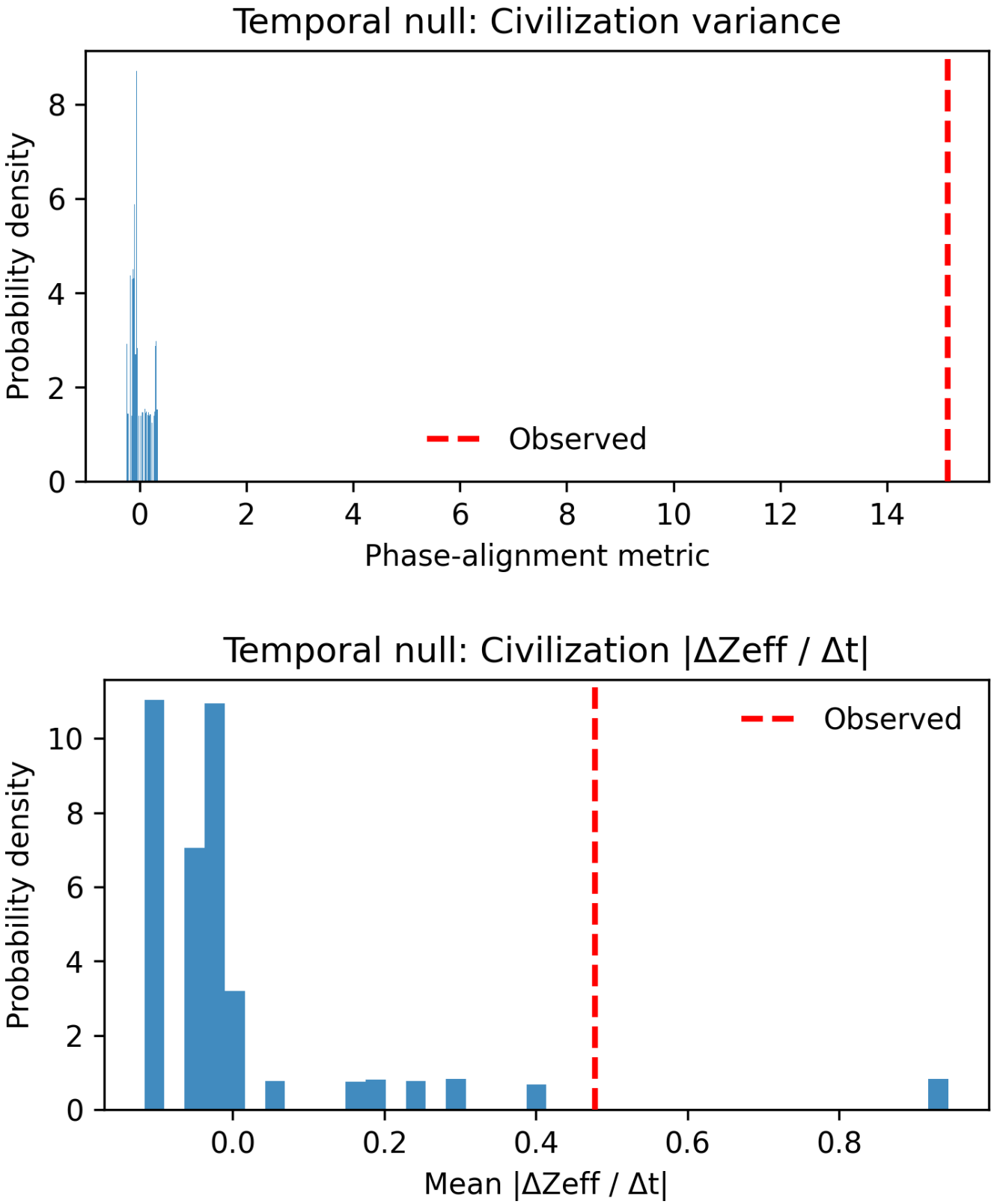

Figure 6: Temporal phase-randomization null tests for early civilization sites. Observed values lie in the tails of the null distributions, indicating non-random temporal alignment.

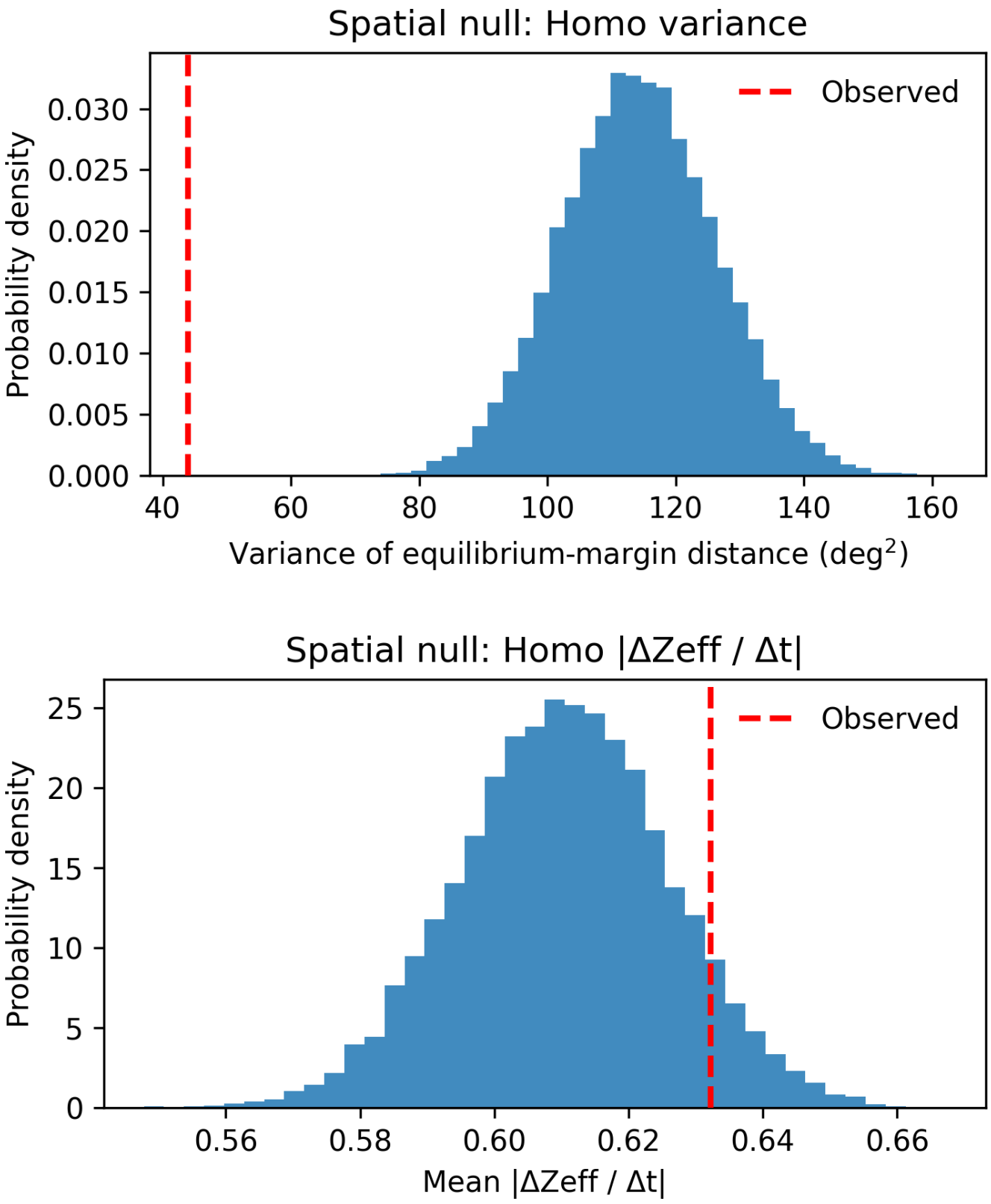

Figure 7: Spatial randomization null tests for early Homo sites.

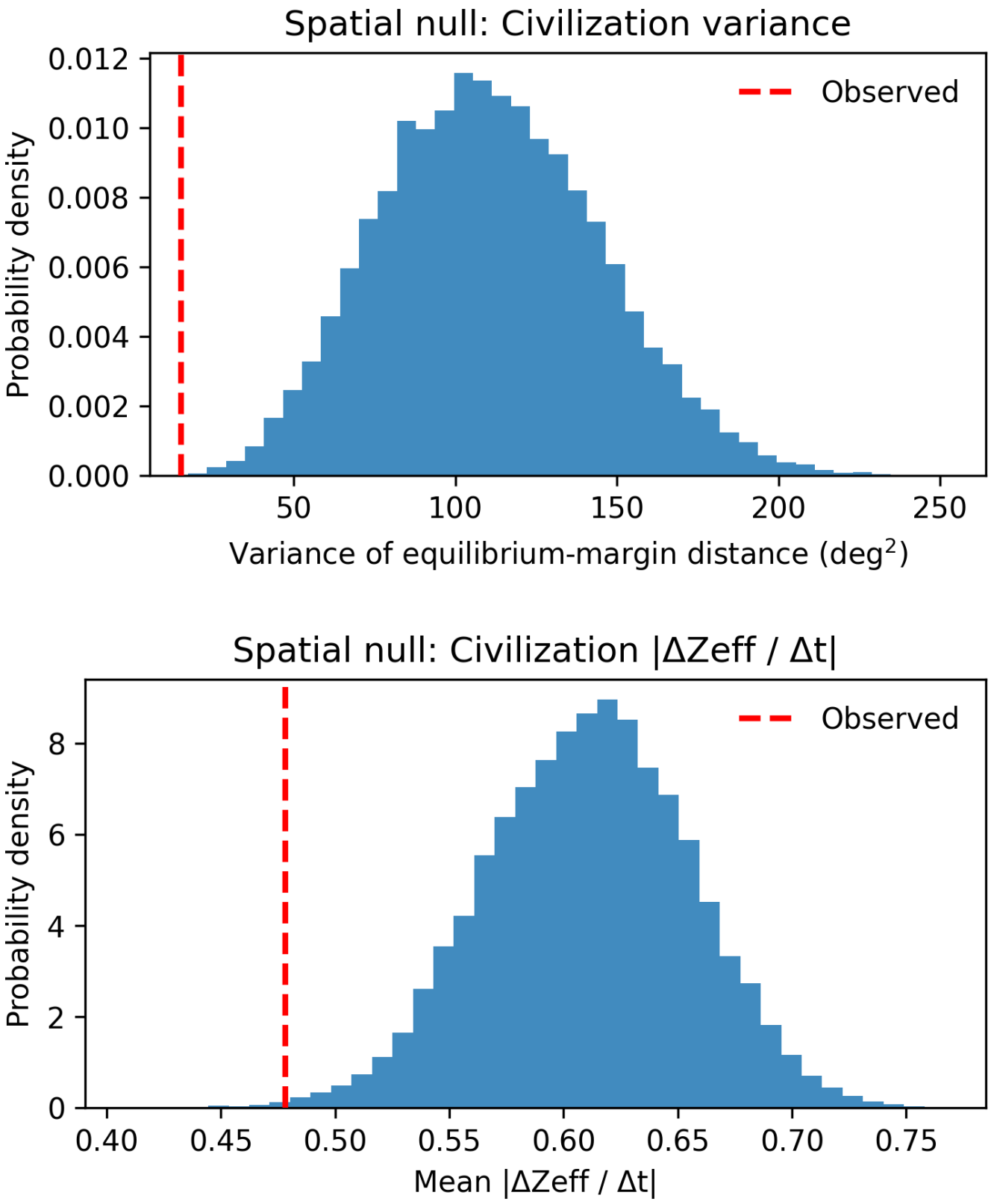

Figure 8: Spatial randomization null tests for early civilization sites.

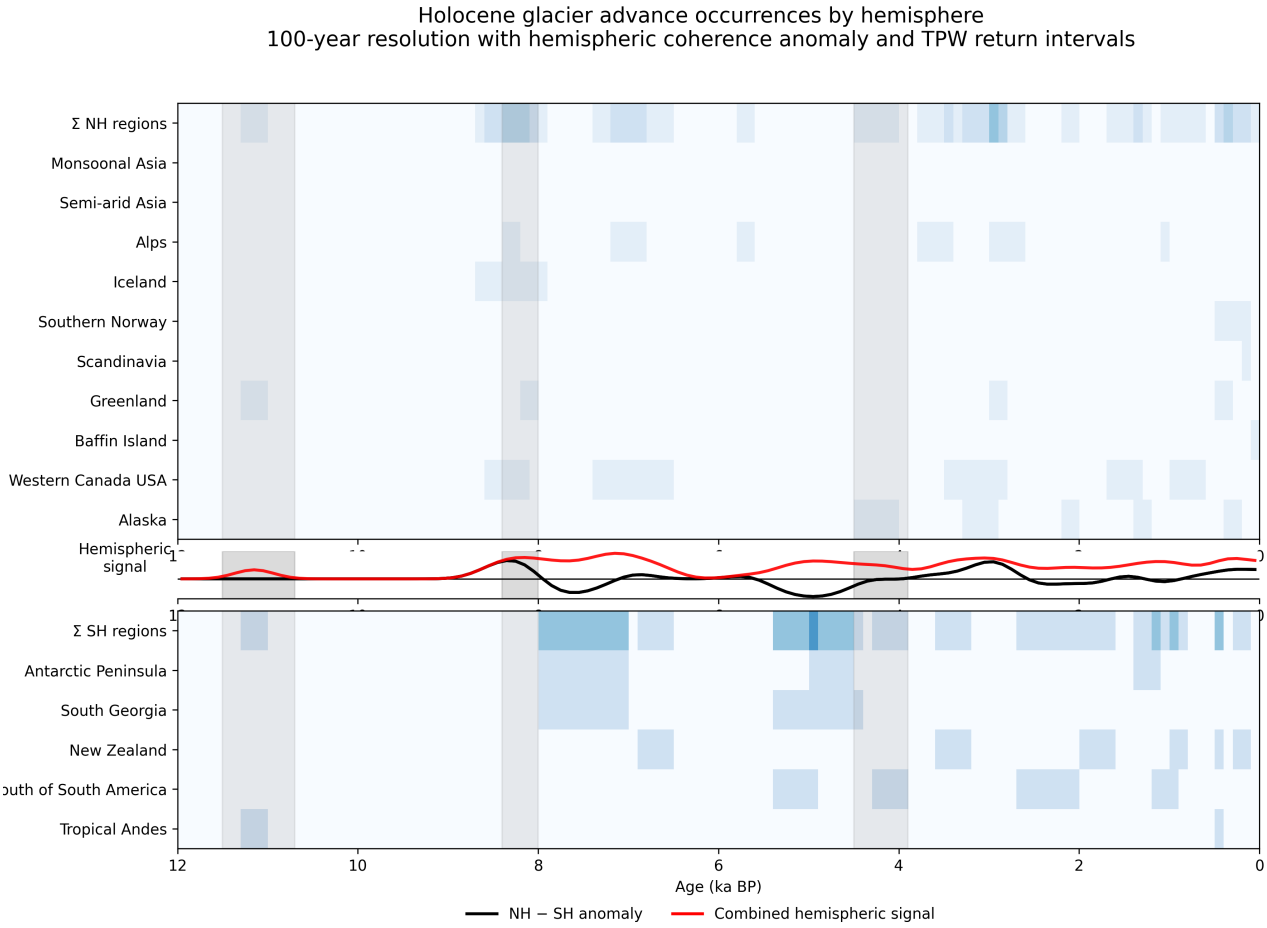

Figure 9: Holocene glacier advance occurrences compiled by Solomina et al. (2015), shown at 100-year temporal resolution and separated by hemisphere. Upper and lower heatmaps display the presence–absence of glacier advances for individual Northern Hemisphere and Southern Hemisphere regions, respectively, with Σ rows indicating the number of regions active in each time bin. Grey vertical bands mark independently defined, event-driven TPW return intervals. The central panel shows two smoothed diagnostics derived from the Σ rows: the black curve represents the signed hemispheric anomaly (NH−SH), while the red curve represents the combined hemispheric signal strength (NH+SH). Peaks in the combined signal coincide with TPW return intervals, indicating episodes of enhanced global coherence in glacier advance activity, whereas hemispheric dominance alternates and is secondary to the timing of these coherent phases.

Table 2: Global geological and geophysical signals that temporally overlap the event-driven TPW step windows used in this study. Each entry lists the broad signal type and the approximate central/affected interval (ka BP).

Step Period (ka BP)	Global geological / geophysical evidence	Date range (ka BP)
11.5–10.7	**Younger Dryas termination:** abrupt Greenland warming and rapid isotopic shift in Greenland ice cores (clear ^{18}O temperature increase at termination).	11.7–11.5
	Meltwater Pulse 1B (MWP-1B): rapid global sea-level rise pulse recorded in far-field coral records and sea-level reconstructions; candidate Antarctic and/or Northern Hemisphere sources.	11.5
	Meltwater Pulse 2A (MWP-2A): rapid global sea-level rise pulse recorded in far-field coral records and sea-level reconstructions; candidate Antarctic and/or Northern Hemisphere sources.	11.0
	Large, near-global CH_4/greenhouse gas excursions and wetland reorganisation: rapid changes in ice-core methane records tied to hydrological/biogeochemical reorganisation.	12.9–11.5 (largest change at termination)
	Bond Event 8: One of nine ice-rafting events carrying coarse-grained rocky debris from Greenland and Iceland to the North Atlantic Ocean during the Holocene Epoch.	
	Pleistocene Megafauna Extinctions: More than 32 genera of large mammals vanished from North America and other continents.	12.0–10.0
8.4–8.0	**8.2 ka event (freshwater forcing):** abrupt Northern Hemisphere cooling, widely observed in ice cores, lake records and marine proxies; linked to catastrophic drainage (Agassiz–Ojibway) and short AMOC weakening.	8.4–8.0 (peak 8.2)
	Sea-level fingerprint / ocean circulation perturbation: sea-level and marine proxy responses consistent with a rapid freshwater pulse and transient ocean circulation change.	8.3–8.1
	Bond Event 5: One of nine ice-rafting events	
	GRIP Deuterium anomaly: One of three abrupt declines punctuating the GRIP excess record (8.2, 4.5, and 0.35 ka BP), suggesting associated reorganizations of the northern high latitudes hydrological cycle.	
4.5–3.9	**4.2 ka event / mid-to-late Holocene aridification:** widespread hydroclimatic anomalies — multi-regional droughts, monsoon weakening, and glacier advances/ice growth signals in multiple mountain ranges and ice cores.	4.5–3.9 (peak ca. 4.2)
	AMOC / North Atlantic SST anomalies and teleconnections: palaeoceanographic reconstructions show cooler North Atlantic SSTs and linked hydroclimatic teleconnections affecting Asia, Africa, and the Mediterranean.	ca. 4.3–4.0
	Bond Event 3: One of nine ice-rafting events	
	GRIP Deuterium anomaly: One of three abrupt declines	

Notes: The table lists broad, globally-expressed geophysical signals that are temporally coincident (overlap) with the event-driven TPW step windows used in this study. These lines of evidence are drawn from high-resolution Greenland ice-core temperature and gas records, coral and far-field sea-level reconstructions, lake and speleothem drought proxies, and palaeoceanographic syntheses.

Primary sources consulted (high-level syntheses and records): Greenland ice-core reconstructions and Younger Dryas temperature analyses; sea-level reconstructions and MWP-1B syntheses; freshwater forcing and AMOC response literature for the 8.2 ka event; Holocene multi-proxy syntheses for the 4.2 ka event. Representative citations (for direct reference): Rasmussen et al. (Greenland ice cores / Younger Dryas), Bard et al. and subsequent MWP1B syntheses, studies linking Agassiz–Ojibway drainage to the 8.2 ka event, and multi-region reviews of the 4.2 ka event and mid-Holocene droughts.